MAGNETIC RESONANCE ELECTRICAL PROPERTIES TOMOGRAPHY (MREPT) BASED ON THE SOLUTION OF THE CONVECTION-REACTION EQUATION

Fatih Suleyman Hafalir[1], Omer Faruk Oran[1], Necip Gurler[1], and Yusuf Ziya Ider[1]

[1]*Electrical and Electronics Engineering, Bilkent University, Ankara, Turkey*

Introduction: Imaging of electrical properties (EP) of tissues (conductivity σ and permittivity ε) using MRI is important to provide diagnostic information about tissues and patient-specific real-time SAR calculation. Magnetic Resonance Electrical Properties Tomography (MREPT) achieves noninvasive electrical property mapping using the measured complex B_1 field at Larmor frequency. Currently available practical MREPT methods [1,2] reconstruct electrical properties within local homogeneous regions where σ and ε values are almost constant. In this study, we propose a novel algorithm named convection-reaction equation based MREPT (cr-MREPT) which reconstructs σ and ε also in transition regions where σ and ε vary. A similar algorithm has been previously proposed for MREIT.[3]

Theory: Starting from the Maxwell's equations, a partial differential equation (Eq. 2) is derived for $\gamma = \sigma + i w\varepsilon$. For birdcage and TEM coils, it is reasonable to neglect the axial H_z component and using this assumption, Eq.3 is derived. Dividing by γ and defining $u=1/\gamma$, we obtain Eq.4 which is in the form of the convection-reaction equation where the coefficients depend on the complex B_1^+ map.

$$-\nabla^2 \boldsymbol{H} = \frac{\nabla\gamma}{\gamma}\times(\nabla\times\boldsymbol{H}) - i\omega\mu\gamma\boldsymbol{H} \quad \text{and} \quad H^+ = \frac{(H_x + iH_y)}{2} \qquad (1)$$

$$-2\nabla^2 H^+ = -2\, i\omega\mu\gamma H^+ + 2\frac{1}{\gamma}\left(\frac{\partial\gamma}{\partial y} - i\frac{\partial\gamma}{\partial x}\right)\left(-i\frac{\partial H^+}{\partial x} - \frac{\partial H^+}{\partial y} - \frac{i}{2}\frac{\partial H_z}{\partial z}\right) - 2\frac{1}{\gamma}\frac{\partial\gamma}{\partial z}\left(\frac{\partial H^+}{\partial z}\right) - \frac{1}{\gamma}\frac{\partial\gamma}{\partial z}\left(\frac{\partial H_z}{\partial x} + i\frac{\partial H_z}{\partial y}\right) \qquad (2)$$

$$-\nabla^2 H^+ = \frac{1}{\gamma}\left(\frac{\partial\gamma}{\partial y} - i\frac{\partial\gamma}{\partial x}\right)\left(-i\frac{\partial H^+}{\partial x} - \frac{\partial H^+}{\partial y}\right) - \frac{1}{\gamma}\frac{\partial\gamma}{\partial z}\left(\frac{\partial H^+}{\partial z}\right) - i\omega\mu\gamma H^+ \qquad (3)$$

$$\nabla u\cdot\mathbf{F} + \nabla^2 H^+ u = i\omega\mu H^+ \quad \text{where} \quad \mathbf{F} = \begin{bmatrix} \partial H^+/\partial x - i\,\partial H^+/\partial y \\ i\,\partial H^+/\partial x + \partial H^+/\partial y \\ \partial H^+/\partial z \end{bmatrix} \qquad (4)$$

($\mathbf{F}$ is called the convective field)

Method: Simulated magnetic field data is generated using COMSOL Multiphysics (COMSOL AB, Sweden) for the phantom shown in Fig.1a. In this phantom two eccentric cylindrical objects with different EPs are placed in a birdcage coil model. The cross-sectional σ and ε distributions are shown in Fig. 1b. For experimental studies, we constructed a rectangular phantom (filled with solution of 1 gr/l $CuSO_4$, 12 gr/l NaCl, σ measured as 1 S/m) which contains a cylindrical bottle (filled with solution of 1 gr/l $CuSO_4$, 2.3 gr/l NaCl, σ measured as 0.4 S/m). All experiments were performed on a 3T MR scanner (Siemens, Erlangen, Germany) using quadrature transmit/receive coil. B_1^+ amplitude map is acquired using double angle method[4] (flip angle = 45° and 90°, TR=2000ms, GRE, 1.6x1.6x5mm, 3 axial slices). B_1^+ phase map is approximated as half of the transceive phase for quadrature birdcage coil and transceive phase is acquired by SE experiment (1.6x1.6x5 mm, SE, TR=2000, 3 axial slices).[1] In simulations and experiments, Laplacian of B_1^+ is calculated using 3 axial slices. A Gaussian filter with kernel size 5 and standard deviation 1 is applied to the measured complex B_1^+ maps. Using simulated and measured B_1^+ magnitude and phase maps, convection-reaction equation (Eq.4) is then solved using finite element method (FEM) to reconstruct u. In order to solve this equation, Dirichlet boundary condition is used, i.e., σ and ε are specified at the boundary.

$$u = \frac{i\omega\mu H^+}{\nabla^2 H^+} \qquad (5)$$

Results: Using simulated B_1^+ map, the solution of Eq.4 gives the σ and ε reconstructions shown in Fig.2a and 2b. In these figures, a spot-like artifact is observed. This artifact is mainly due to the numerical errors introduced by the region where the modulus of the convective field (in Eq.4) is nearly zero (shown in Fig.1c). This region is referred to as the Low Convection Field (LCF) region. To eliminate the spot-like artifact, first we determine the LCF region by observing the convective field, and in this region we use Eq.5 which is derived by ignoring the convection term in Eq.4. Then, we solve Eq.4 by providing the σ and ε found from Eq.5 in the LCF region as a-priori knowledge. The resultant reconstructed σ and ε, shown in Fig.2c and 2d, do not have spot-like artifacts. Using experimentally obtained B_1^+ map (Fig.3b and 3c), σ is reconstructed using three different methods as shown in Fig.3d-3f: (i) Eq.4 is solved directly in which case the spot-like artifact is again observed. (ii) Eq.4 is solved providing a-priori knowledge in the LCF region and thus the spot-like artifact is eliminated. (iii) Eq.5 is used in all regions (Wen's method[1]) and reconstruction errors are significantly large around the boundary of the bottle where σ changes.

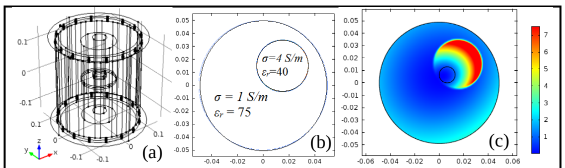

Fig. 1. (a) Simulation phantom, (b) simulated actual σ and ε_r, (c) modulus of convective field (black circle shows LCF region)

Discussion and Conclusion: Using both the simulated and the experimental data, reconstructions using cr-MREPT are successful in all regions, including the σ and ε transition regions. Since Laplacian operation amplifies noise, cr-MREPT method is sensitive to noise and the quality of reconstruction results depends on SNR of B_1^+ complex maps. We are currently working on decreasing the noise effect on reconsructions and on increasing SNR of B_1^+ maps. In addition, in order to eliminate spot-like artifacts, we are working on acquiring multiple sets of B_1^+ data with different LCF regions and combining them while solving Eq.4.[3]

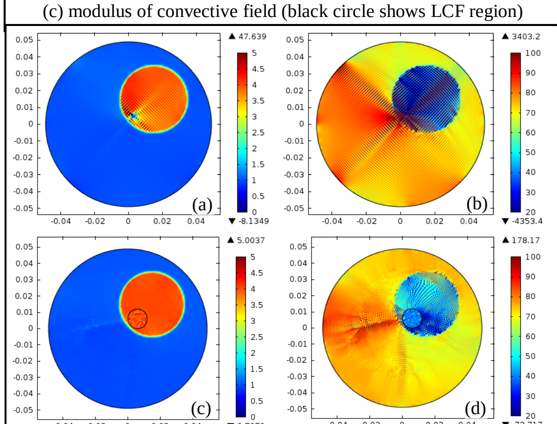

Fig. 2. Simulation results of cr-MREPT method, reconstructed (a) conductivity and (b) permittivity. Reconstructed (c) conductivity and (d) permittivity when the artifact is eliminated.

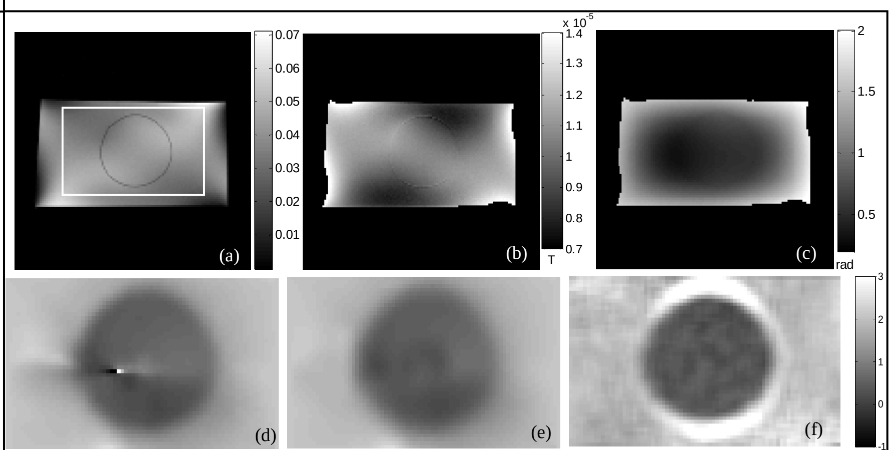

Fig 3. (a) SE magnitude (white rectangle shows the region of interest), (b) B_1^+ magnitude, (c) B_1^+ phase image. Reconstructed conductivity: (d) cr-MREPT, (e) cr-MREPT when the artifact is eliminated, (f) Wen's method.

Acknowledgements: This work is supported by TUBITAK 111E090 grant. Experimental data are acquired using the facilities of UMRAM, Bilkent University, Ankara

References: [1]Wen, Proc. SPIE 2003;5030:471-77. [2]Katscher U et al, *IEEE Trans Med Imaging* 2009;28:1365-74. [3]Oran et al, Phys Med Biol. 2012;57:5113-40. [4]Stolllberger et al, Magn. Reson. Med. 1996;35:246-51.